



HAL
open science

InAs/InP(001) quantum dots emitting at $1.55\mu\text{m}$ grown by low-pressure metalorganic vapor-phase epitaxy

A. Michon, Guillaume Saint-Girons, G. Beaudoin, I. Sagnes, L. Largeau, G. Patriarche

► To cite this version:

A. Michon, Guillaume Saint-Girons, G. Beaudoin, I. Sagnes, L. Largeau, et al.. InAs/InP(001) quantum dots emitting at $1.55\mu\text{m}$ grown by low-pressure metalorganic vapor-phase epitaxy. Applied Physics Letters, 2005, 87 (25), pp.253114. 10.1063/1.2150271 . hal-01939897

HAL Id: hal-01939897

<https://hal.science/hal-01939897>

Submitted on 8 Dec 2022

HAL is a multi-disciplinary open access archive for the deposit and dissemination of scientific research documents, whether they are published or not. The documents may come from teaching and research institutions in France or abroad, or from public or private research centers.

L'archive ouverte pluridisciplinaire **HAL**, est destinée au dépôt et à la diffusion de documents scientifiques de niveau recherche, publiés ou non, émanant des établissements d'enseignement et de recherche français ou étrangers, des laboratoires publics ou privés.

Copyright

InAs/InP(001) quantum dots emitting at 1.55 μm grown by low-pressure metalorganic vapor-phase epitaxy

A. Michon, G. Saint-Girons,^{a)} G. Beaudoin, I. Sagnes, L. Largeau, and G. Patriarche
Laboratoire de Photonique et de Nanostructures, Route de Nozay, 91460, Marcoussis, France

(Received 31 May 2005; accepted 14 November 2005; published online 16 December 2005)

In this letter, we report on the structural and optical properties of self-assembled InAs quantum dots (QDs) directly grown on InP(001) by low-pressure metalorganic vapor-phase epitaxy. Transmission electron microscopy reveals defect-free diamond-shaped QDs with a density as high as $2.5 \times 10^{10} \text{ cm}^{-2}$. The QD photoluminescence exhibits an intense peak centered around 1.58 μm (785 meV) at room temperature. Changing the growth rate allows one to control the QD density, while maintaining an intense emission centered at this wavelength. These promising results open the way for the realization of efficient InAs/InP(001) QD-based devices, such as lasers or single-photon sources. © 2005 American Institute of Physics. [DOI: 10.1063/1.2150271]

Nanosized self-assembled quantum dots (QDs) fabricated in the Stranski-Krastanov growth mode have attracted great interest in the last two decades. The main causes of this infatuation is the strong charge-carrier confinement inside the QDs, which leads to a discrete density of electronic states, and to a high robustness against defects that might surround the QDs layers. These original properties have driven a number of fundamental physical studies and have been exploited in the fabrication of novel high-performance devices, such as low-threshold and temperature-insensitive 1.3 μm edge-emitting lasers,¹ as well as promising single-photon sources for quantum cryptography applications.² More recently, efficient emission at the telecom wavelength of 1.55 μm has been obtained from InAs/InP QDs. This opens the way for the realization of efficient QD-based devices for long-range telecommunications applications. Various studies, involving molecular beam epitaxy^{3,4} and chemical beam epitaxy⁵ growth of InAs QDs on exactly (001)-oriented InP substrates, demonstrate the difficulty in obtaining real three-dimensional QDs using these high-vacuum growth techniques. Many authors have reported the formation of nanostructures strongly elongated along the [1–10] directions; namely, “quantum dashes” or “quantum sticks.” To circumvent this difficulty, a few groups have used (311)B-oriented InP substrates.⁶ However, these substrates are not compatible with the standard processes used in the fabrication of optoelectronic devices. Metalorganic vapor-phase epitaxy (MOVPE) has also been used for the growth of InAs/InP(001) QDs. Some early studies have shown that MOVPE allows one to obtain QDs rather than quantum dashes.^{7,8} The MOVPE, particularly well suited for industrial applications, therefore appears as an appealing alternative to high-vacuum techniques for the fabrication of high quality InAs/InP QDs. Some groups have grown InAs QDs on a InGaAsP buffer layer lattice matched to InP. These QDs present very good optical properties, and densities as high as $5.6 \times 10^{10} \text{ cm}^{-2}$. However, their emission presents a large full width at half-maximum (FWHM), of the order of 100 meV at room temperature.⁹ It has also been proposed to grow InAs/InP(001) QDs on a thin GaAs underlayer. Thus, Anan-

tathanasarn *et al.*¹⁰ have obtained intense tunable QD emission around 1.55 μm , with a large FWHM of approximately 100 meV at room temperature. Such large FWHM are prejudicial for the performance of QD-based lasers.

In this letter, we report on the structural and optical properties of high-density and defect-free self-assembled InAs QDs grown on exactly (001)-oriented InP substrates by low-pressure MOVPE presenting an intense narrow emission around 1.58 μm at room temperature.

All samples were grown in a low-pressure MOVPE system using hydrogen as carrier gas at a work pressure of 60 Torr. Standard precursors [arsine, phosphine, and trimethylindium (TMI)] were used for the growth of the QD samples. The growth sequence is as follows: after a 150 nm thick InP buffer layer deposited at 625 °C on an exactly (001)-oriented InP substrate, the growth temperature was lowered to 530 °C for the QD deposition. The QDs were formed by depositing 4 monolayers (ML) of InAs, at growth rates of 0.5 and 0.2 ML s^{-1} (TMI flow rates of 0.38 and 0.15 $\mu\text{mol s}^{-1}$) for samples A and B, respectively, and an arsine flow rate of 6 sccm. Finally, a 40 nm thick InP capping layer was grown over the QDs at 530 °C. The InAs growth rate was carefully determined using transmission electron microscopy (TEM) and x-ray diffraction experiments. The final composition of the alloy forming the QDs is approximately $\text{InAs}_{0.96}\text{P}_{0.04}$, due to As/P exchange.

The TEM plane views shown in the following were taken under 001 bright-field zone-axis and 220 dark-field conditions. Photoluminescence (PL) spectra of the samples were also recorded. The optical excitation was supplied by a 532 nm laser focused down to a 100 μm diameter spot on the sample. The PL signal was detected by a cooled Ge detector and a lock-in amplifier. All the spectra were recorded using a low excitation power of 30 μW , in order to avoid ground state saturation. Under these excitation conditions, if we assume a charge-carrier lifetime of 4 ns,¹¹ each QD contains on average less than 0.1 charge carriers, well below the saturation level for the ground state.

A 220 dark-field TEM plane view of sample A is shown in Fig. 1(a). This sample contains well-defined three-dimensional dislocation-free QDs, with a density of 2.5×10^{10} QDs per cm^2 . The inset of Fig. 1(a) presents a typical QD (001 bright-field imaging conditions). It is diamond

^{a)}Electronic mail: Guillaume.saint-girons@lpn.cnrs.fr

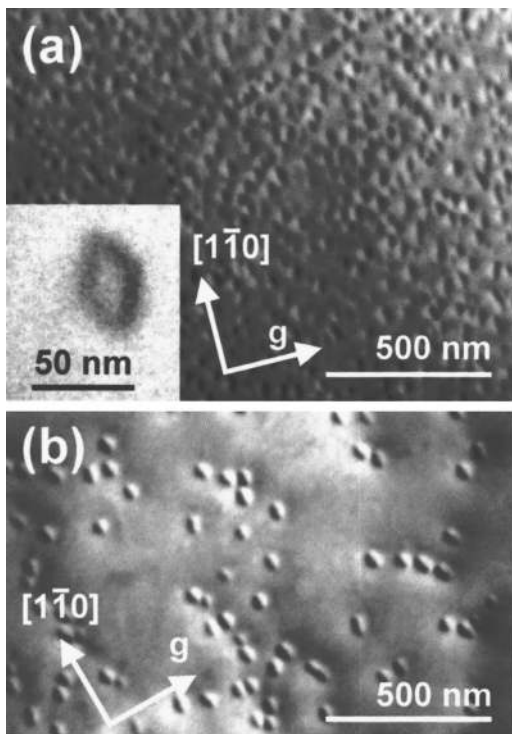


FIG. 1. (a) TEM plane view (220 dark field) of sample A (0.5 ML s^{-1}). The QDs are slightly elongated along $[1-10]$. The average largest dimension is $d_{[1-10]}=51 \text{ nm}$, and the average smallest dimension is $d_{[110]}=28 \text{ nm}$. The inset presents a QD (001 bright-field imaging conditions). (b) TEM plane view (220 dark field) of sample B (0.2 ML s^{-1}). The density is 5 times smaller than for sample A, and the average smallest dimension increases to $d_{[110]}=33 \text{ nm}$.

shaped, slightly elongated along the $[1-10]$ direction. The sides of the QDs correspond to the $[1-30]$ and $[3-10]$ directions. The same type of diamond-shaped QDs have recently been observed by Hwang *et al.*¹² in the case of uncapped QD layers grown on a thin $\text{In}_{0.53}\text{Ga}_{0.47}\text{As}$ interlayer. From a statistical analysis, over about 100 objects observed in 001 bright-field imaging conditions, we estimated the dimensions of the QDs: the average largest dimension (along $[1-10]$) is $d_{[1-10]}=51 \text{ nm}$, and the average smallest dimension (along $[110]$) is $d_{[110]}=28 \text{ nm}$. The corresponding size dispersions are 17% for $d_{[1-10]}$ and 11% for $d_{[110]}$.

Figure 1(a) shows that the QD repartition over the surface is not homogeneous: part of the QD ensemble tends to form quasiparallel dense lines regularly spaced by approximately $1.4 \mu\text{m}$. We attributed this phenomenon to an enhancement of the QD nucleation along the atomic steps of the buffer or wetting layer.¹³

The 220 dark-field TEM plane view of sample B, grown at smaller growth rate than sample A, is shown in Fig. 1(b). The QDs of this sample present the same diamond shape and the same orientation as the ones of sample A. The reduction of the growth rate leads to a reduction of the QD density to $4.5 \cdot 10^9 \text{ cm}^{-2}$ for sample B. The average dimensions of the QDs of sample B are $d_{[1-10]}=53 \text{ nm}$ and $d_{[110]}=33 \text{ nm}$, with size dispersions of 13% and 12%, respectively. $d_{[110]}$ is 5 nm larger for sample B than for sample A. Note that due to the imaging conditions, the accuracy of the size measurement is not the same for both dimensions of the QDs. In fact, the contrast under 001 bright-field imaging conditions is driven mainly by the strain around the base of the QDs. This con-

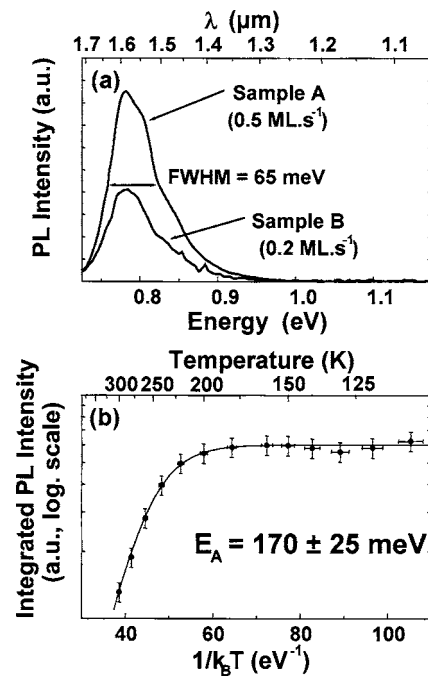


FIG. 2. (a) PL spectra of samples A and B (intensity $\times 3$) taken at room temperature. Both samples exhibit an intense PL peak centered around $1.58 \mu\text{m}$. (b) Arrhenius plot of the PL integrated intensity (circles) with experimental error bars, and fit (solid line) with an activation energy $E_A = 170 \pm 25 \text{ meV}$.

trast is better defined in the obtuse corners of the QDs, leading to a more accurate measurement of the $d_{[110]}$ dimension. We estimated the accuracy of the size measurement to be $\pm 2 \text{ nm}$ for the $d_{[110]}$ dimension, and $\pm 5 \text{ nm}$ for the $d_{[1-10]}$ dimension. Note, moreover, that for both samples A and B, cross-sectional TEM views (not shown here) reveal the presence of a 0.8 nm thick wetting layer under the QDs.

The fact that an increase in the growth rate results in a increase of the QD density is a well known kinetic effect, already observed for InAs QDs grown on GaAs substrate.¹⁴ It is also well known that an increase of the QD growth rate leads to a decrease of their size. In our QD samples, the largest dimension $d_{[1-10]}$ of the QDs is less affected than the smallest dimension by a variation of the growth rate. Further studies are required in order to clearly understand this effect.

The PL spectra of samples A and B recorded at room temperature are compared in Fig. 2(a). The PL peaks of both samples are centered around $1.58 \mu\text{m}$, and present a FWHM of 65 meV . This is consistent with the fact that the emission energy of a QD ensemble depends mainly on the average height of the QDs, and not on their lateral size.¹⁵ Thus, the reduction of $d_{[110]}$ induced by an increase of the growth rate has no effect on the PL spectra. The integrated PL intensity of sample A is approximately 6 times larger than the one of sample B. We attributed this increase of the PL intensity to an enhancement of the charge-carriers, capture in the QDs due to the increase of the QD density. At higher excitation powers (not shown here), the PL spectrum of sample B exhibits a peak centered at 1.04 eV corresponding to the emission of the wetting layer of the QDs. This peak was not observed for sample A, due to the high QD density in this sample, that leads to a fast trapping of the charge carriers in the QDs.

We also performed temperature-dependent PL experiments for sample A. The evolution of the QD integrated intensity is plotted in Fig. 2(b). The PL intensity at 300 K is only five times lower than that at 80 K, indicating the high optical quality of our QDs. In the low-temperature range, the PL intensity is constant. It starts to decrease for temperatures above 160 K due to the onset of thermally activated nonradiative recombinations. A rate equation model,¹⁶ describing the charge-carrier recombination in QD layers, was used to fit the experimental data of Fig. 2(b). The best fit (continuous line) was obtained for an activation energy of the nonradiative recombinations E_A of 170 meV. The precision of this value, taking into account experimental errors, is approximately ± 25 meV. This simple analysis does not allow us to reach a conclusion on the origin of the nonradiative recombinations, which is beyond the topic of this study. However, some interesting discussion can be made on the basis of the results presented in Ref. 17. In this letter the authors derive the band structure of InAs/InP QDs presenting size and shape very similar to our QDs. In particular, they show that the confinement energies for electrons (holes) in the QDs is 70 meV (427 meV) with respect to the wetting layer. Based on these conclusions, the confinement energy of holes is much higher than the activation energy derived from Fig. 2(b). The nonradiative recombinations in our QDs can therefore either be related to the thermionic escape of the electrons to the wetting layer, and their further nonradiative recombination on defects in this layer, or to a correlated escape of electrons and holes out of the QDs. This latter hypothesis can be considered only in the case where the charge carriers trapped in the QDs present a collective Fermi level,¹⁸ which is a reasonable assumption for a dense QD array at room temperature.¹⁹ In this case, the activation energy of the nonradiative recombinations is equal to the half of the total confinement energy of the charge carriers, that is, approximately 250 meV. This value is slightly larger than the one derived from Fig. 2(b), but further studies are required to definitively conclude on the origin of the nonradiative recombinations in our QDs.

To conclude, our results show that MOVPE is well suited to obtain well defined InAs/InP(001) QDs. Our growth conditions allow the control of the QD density, while maintaining a strong emission centered around $1.58 \mu\text{m}$. The dependence of the QD size and density on the growth rate

indicates that the growth of the QDs is predominantly driven by kinetic phenomena.

We obtained a QD density of $2.5 \times 10^{10} \text{ cm}^{-2}$. This density is suitable for the realization of QD-based lasers, and could be further increased by increasing the growth rate. On the other hand, further decrease of the growth rate could allow the fabrication of ultra-low-density QD arrays for single-photon source applications.

This work was supported by the SANDIE EC Network of Excellence, by SESAME project no. 1377, by the Région Ile de France, and by the Conseil Général de l'Essonne.

- ¹O. B. Shchekin, J. Ahn, and D. G. Deppe, *Electron. Lett.* **38**, 712 (2003).
- ²E. Moreau, I. Robert, L. Manin, V. Thyerry-Mieg, J. M. Gerard, and I. Abram, *Phys. Rev. Lett.* **87**, 183601 (2001).
- ³M. Gendry, C. Monat, J. Brault, P. Regreny, G. Hollinger, B. Salem, G. Guillot, T. Benyattou, C. Bru-Chevalier, G. Bremond, and O. Marty, *J. Appl. Phys.* **95**, 4761 (2004).
- ⁴L. Gonzalez, J. M. Garcia, R. Garcia, F. Briones, and J. Martinez-Pastor, *Appl. Phys. Lett.* **76**, 1104 (2000).
- ⁵Q. Gong, R. Nötzel, P. J. van Veldhoven, and J. H. Wolter, *J. Cryst. Growth* **278**, 67, (2005).
- ⁶S. Fréchengues, N. Bertru, V. Drouot, B. Lambert, S. Robinet, S. Loualiche, D. Lacombe, and A. Ponchet, *Appl. Phys. Lett.* **74**, 3356 (1999).
- ⁷H. Marchand, P. Desjardins, S. Guillon, J.-E. Paultre, Z. Bougrioua, R. Y.-F. Yip, and R. A. Masut, *Appl. Phys. Lett.* **71**, 527 (1997).
- ⁸N. Carlsson, T. Junno, L. Montelius, M.-E. Pistol, L. Samuelson, and W. Seifert, *J. Cryst. Growth* **191**, 347 (1998).
- ⁹K. Kawaguchi, M. Ekawa, A. Kuramata, T. Akiyama, H. Ebe, M. Sugawara, and Y. Arakawa, *Appl. Phys. Lett.* **85**, 4331 (2004).
- ¹⁰S. Anantathanasarn, R. Nötzel, P. J. van Veldhoven, T. J. Eijkemans, and J. H. Wolter, *J. Appl. Phys.* **98**, 13503 (2005).
- ¹¹W. G. Jeong, P. Daniel Dapkus, U. H. Lee, J. S. Yim, D. Lee, and B. T. Lee, *Appl. Phys. Lett.* **78**, 1171 (2001).
- ¹²H. Hwang, S. Yoon, H. Kwon, E. Yoon, H.-S. Kim, J. Y. Lee, and B. Cho, *Appl. Phys. Lett.* **85**, 6383 (2004).
- ¹³R. Leon, T. Senden, Y. Kim, C. Jagadish, and A. Clark, *Phys. Rev. Lett.* **78**, 4942 (1997).
- ¹⁴P. B. Joyce, T. J. Kryzewski, G. R. Bell, T. S. Jones, S. Malik, D. Childs, and R. Murray, *Phys. Rev. B* **62**, 10891 (2000).
- ¹⁵S. Sauvage, Ph.D. thesis, University of Paris-Sud Orsay, France, 1998.
- ¹⁶G. Saint-Girons and I. Sagnes, *Appl. Phys. Lett.* **91**, 10115 (2002).
- ¹⁷H. Petterson, R. J. Warburton, J. P. Kotthaus, N. Carlsson, W. Seifert, M. E. Pistol, and L. Samuelson, *Phys. Rev. B* **60**, R11289 (1999).
- ¹⁸P. Michler, A. Hangleiter, M. Moser, M Geiger, and F. Scholtz, *Phys. Rev. B* **46**, 7280, (1992).
- ¹⁹A. E. Zhukov, V. M. Ustinov, A. Y. Egorov, A. R. Kovsh, A. F. Tatsulnikov, N. N. Ledentsov, S. V. Zaitsev, N. Y. Gordeev, P. S. Kopev, and Z. I. Alferov, *Jap. J. Appl. Phys. I* **36**, 4216 (1997).